Report

Current Biology

Somatosensory Cortex Efficiently Processes Touch Located Beyond the Body

Highlights

- Human sensorimotor system rapidly localizes touch on a hand-held tool
- Brain responses in a deafferented patient suggest vibrations encode touch location
- Somatosensory cortex efficiently extracts touch location from the tool's vibrations
- Somatosensory cortex reuses neural processes devoted to mapping touch on the body

Authors

Luke E. Miller, Cécile Fabio, Valeria Ravenda, ..., Nadia Bolognini, Vincent Hayward, Alessandro Farnè

Correspondence

l.miller@donders.ru.nl

In Brief

Using electroencephalography, Miller et al. found that where a hand-held tool is touched is rapidly represented by the dynamics of sensorimotor cortices. Primary somatosensory cortex efficiently extracts location information encoded by the tool's vibratory patterns. The brain reuses neural processes initially devoted to mapping touch on the body.

Miller et al., 2019, Current Biology *29*, 4276–4283
December 16, 2019 © 2019 The Authors. Published by Elsevier Ltd.
https://doi.org/10.1016/j.cub.2019.10.043

CellPress

Current Biology
Report

Somatosensory Cortex Efficiently Processes Touch Located Beyond the Body

Luke E. Miller,[1,2,3,9,*] Cécile Fabio,[1,2] Valeria Ravenda,[1,2,6] Salam Bahmad,[1,2] Eric Koun,[1,2,3] Romeo Salemme,[1,2,3] Jacques Luauté,[1,2,3] Nadia Bolognini,[6,7] Vincent Hayward,[4,5] and Alessandro Farnè[1,2,3,8]
[1]Integrative Multisensory Perception Action & Cognition Team—ImpAct, Lyon Neuroscience Research Center, INSERM U1028, CNRS U5292, 16 Avenue Doyen Lépine, Bron 69676, France
[2]University of Lyon 1, 43 Boulevard du 11 Novembre 1918, Villeurbanne 69100, France
[3]Hospices Civils de Lyon, Neuro-immersion, 16 Avenue Doyen Lépine, Bron 69676, France
[4]Sorbonne Université, Institut des Systèmes Intelligents et de Robotique (ISIR), 4 Place Jussieu, Paris 75005, France
[5]Centre for the Study of the Senses, School of Advanced Study, University of London, Senate House, Malet Street, London WC1E 7HU, UK
[6]Department of Psychology & Milan Center for Neuroscience—NeuroMi, University of Milano Bicocca, Building U6, 1 Piazza dell'Ateneo Nuovo, Milan 20126, Italy
[7]Laboratory of Neuropsychology, IRCSS Istituto Auxologico Italiano, 28 Via G. Mercalli, Milan 20122, Italy
[8]Center for Mind/Brain Sciences, University of Trento, 31 Corso Bettini, Rovereto 38068, Italy
[9]Lead Contact
*Correspondence: l.miller@donders.ru.nl
https://doi.org/10.1016/j.cub.2019.10.043

SUMMARY

The extent to which a tool is an extension of its user is a question that has fascinated writers and philosophers for centuries [1]. Despite two decades of research [2–7], it remains unknown how this could be instantiated at the neural level. To this aim, the present study combined behavior, electrophysiology and neuronal modeling to characterize how the human brain could treat a tool like an extended sensory "organ." As with the body, participants localize touches on a hand-held tool with near-perfect accuracy [7]. This behavior is owed to the ability of the somatosensory system to rapidly and efficiently use the tool as a tactile extension of the body. Using electroencephalography (EEG), we found that where a hand-held tool was touched was immediately coded in the neural dynamics of primary somatosensory and posterior parietal cortices of healthy participants. We found similar neural responses in a proprioceptively deafferented patient with spared touch perception, suggesting that location information is extracted from the rod's vibrational patterns. Simulations of mechanoreceptor responses [8] suggested that the speed at which these patterns are processed is highly efficient. A second EEG experiment showed that touches on the tool and arm surfaces were localized by similar stages of cortical processing. Multivariate decoding algorithms and cortical source reconstruction provided further evidence that early limb-based processes were repurposed to map touch on a tool. We propose that an elementary strategy the human brain uses to sense with tools is to recruit primary somatosensory dynamics otherwise devoted to the body.

RESULTS AND DISCUSSION

In somatosensory perception, there is evidence in many species that intermediaries are treated like non-neural sensory extensions of the body [9]. For example, some spiders actively use their web as an extended sensory "organ" to locate prey [10]. Analogously, humans can use tools to sense the properties of objects from a distance [11–13], such as when a blind person uses a cane to probe the surrounding terrain. This sensorimotor ability is so advanced that humans can almost perfectly localize touch on the surface of a tool [7], suggesting a strong parallel with tactile localization on the body. Characterizing the neural dynamics of tool-extended touch localization provides us with a compelling opportunity to investigate the boundaries of somatosensory processing and hence the question of *sensory embodiment*: to what extent does the human brain treat a tool like an extended sensory organ?

From a theoretical perspective [7], the sensory embodiment of a tool predicts that—as is the case with biological sense organs—the cerebral cortex (1) rapidly extracts location-based information from changes in a tool's sensory-relevant mechanical state (e.g., vibrations) and (2) makes this information available to the somatosensory system in an efficient manner. The peripheral code for touch location is likely different for skin (e.g., a place code) and tools (e.g., a temporal code) [7]. Transforming a temporal to a spatial code—a necessary step for tool-extended localization—is a non-trivial task for the brain. We predict that, to do so efficiently, (3) the brain repurposes low-level processing stages dedicated to localizing touch on the body to localize touch on a tool. Direct evidence for sensory embodiment requires understanding how the structural dynamics of tools couple to the neural dynamics of the cortex. Such evidence can be obtained using neuroimaging methods with high temporal resolution. To this aim, we combined electroencephalography (EEG) and computational modeling to test the aforementioned predictions.

 © 2019 The Authors. Published by Elsevier Ltd.
This is an open access article under the CC BY-NC-ND license (http://creativecommons.org/licenses/by-nc-nd/4.0/).

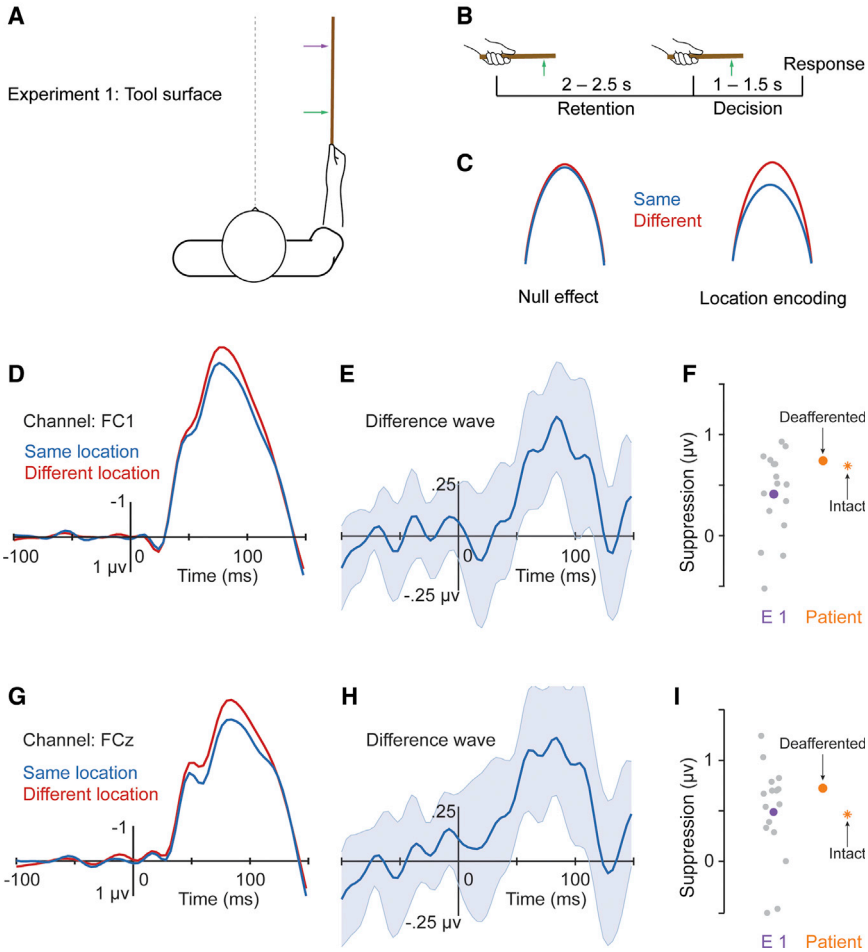

Figure 1. Rapid Processing of Object Location During Tool-Extended Sensing

(A) Participants (n = 16) performed a 2-interval delayed match-to-sample task for touches applied at two locations (colored arrows) on the surface of a tool held in their right hand. This task forced participants to discriminate where the tool was touched (see STAR Methods).

(B) Trial structure of the delayed match-to-sample task. For presentation purposes, only a portion of the rod is shown. Green arrows represent where the rod was hit.

(C) Idealized possible results for a single SEP: repetition suppression in the amplitude of the evoked potential (right) indicates location encoding at that specific stage of somatosensory processing.

(D–I) Representative results are shown for channel FC1 (D–F) and channel FCz (G–I). In both, we found a significant reduction in SEP amplitude (D and G) when the hit was at the same location (blue) compared to a different location (red).

(E and H) The difference waves (different–same) clearly show rapid suppression in both channels. Shaded areas represent the 95% confidence interval.

(F and I) Individual differences for the suppression (average between 52 and 108 ms) at both channels from experiment 1 (mean, purple dot; individuals, gray dot) and from the deafferented participant, DC (orange dots). The suppression observed in DC was on the high end compared to our healthy participants.

See also Figures S1, S2, and S3 and Table S1.

The Cerebral Cortex Rapidly Processes Where a Tool Was Touched

In an initial experiment (n = 16), participants localized touches applied on the surface of a 1-m wooden rod (Figure 1A) while we recorded their cortical dynamics using EEG. We designed a delayed match-to-sample task that forced participants to compare the location of two touches (delivered via solenoids; Figure S1A) separated in time (Figure 1B). If the two touches were felt to be in different locations, participants made no overt response. If they were felt to be in the same location, participants used a pedal with their ipsilateral left foot to report whether the touches were close or far from their hand. Participants never used the rod before the experiment and never received performance feedback. As a result, participants had to rely on preexisting internal models of tool dynamics [14]. Regardless, accuracy was near ceiling for all participants (mean: 96.4% ± 0.71%; range: 89.7%–99.5%), consistent with our prior finding [7].

When a stimulus feature is repeatedly presented to a sensory system, the responses of neural populations representing that feature are suppressed [15]. Effects of repetition are a well-accepted method for timestamping when specific features in a complex input are extracted [16]. Repetition paradigms have previously been used to characterize how sensory signals are mapped by sensorimotor cortices [17–20]. Our experimental paradigm allowed us to leverage these repetition suppression effects to characterize when the brain extracted where a rod has been touched. Specifically, the amplitude of evoked brain responses reflecting the processing of impact location will be reduced if the rod is hit at the same location twice in a row compared to two distinct locations (Figure 1C).

We first characterized the cortical dynamics of tool-extended touch localization. Touching the surface of the rod led to widespread evoked responses over contralateral regions (Figures S1 and S3), starting ~24 ms after contact (Figure S1B); this time course is consistent with the known conduction delays between upper limb nerves and primary somatosensory cortex [21]. A nonparametric cluster-based permutation analysis identified significant location-based repetition suppression in a cluster of sensorimotor electrodes between 48 and 108 ms after contact ($p = 0.003$; Figures 1D–1I, S1C, S1D, and S3; Table S1). This cluster spanned two well-characterized processing stages previously identified for touch on the body: (1) recurrent sensory processing within primary somatosensory (SI) and motor (MI) cortices between 40 and 60 ms after stimulation [22], which has been implicated in spatial processing [23, 24], and (2) feedforward and feedback processing between SI, MI, and posterior parietal regions between 60 and 100 ms after stimulation [25, 26], proposed to contribute to transforming a sensory map into a higher-level spatial representation [18, 27]. This suppression

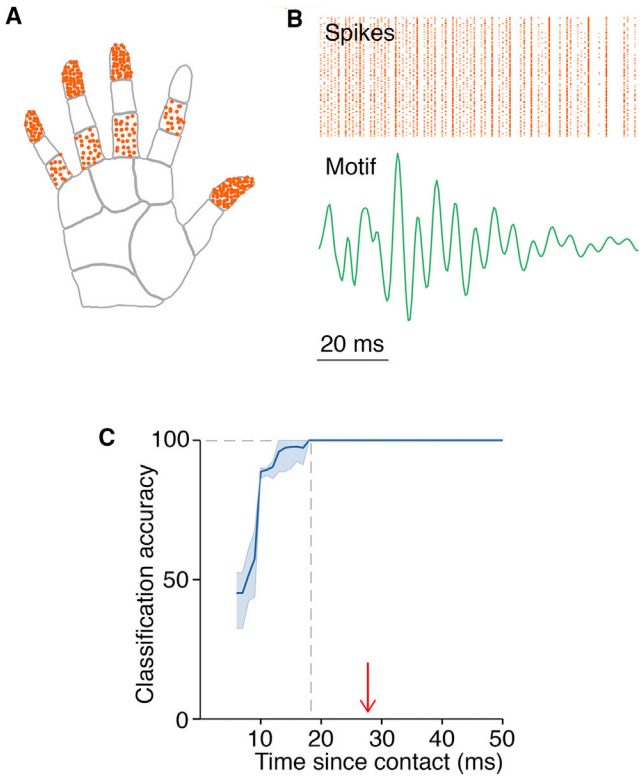

Figure 2. Afferent Simulations Demonstrated Efficient Encoding of Location During Tool-Extended Sensing

(A) We used a skin-neuron model (TouchSim) to simulate a population of 286 Pacinian corpuscles (PCs) in the hand.

(B) We simulated PC spikes (orange ticks) in response to a location-specific vibratory motif (green curve).

(C) Given the spike timing of the PC population, we could decode location with 100% accuracy given a window size of 18 ms (gray dashed line). We took this value to represent the minimal information needed to extract contact location if somatosensory encoding was maximally efficient. The red arrow indicates what we actually observed after removing the 20-ms conduction delay between the periphery and SI [21]. Shaded regions represent the range of accuracy for 100 permutations.

See also Figure S1.

was too quick to reflect signals related to motor preparation/inhibition, which generally occur ~140 ms after touch [28].

Location-based Repetition Suppression Is Driven by Vibratory Signals

We previously suggested that, during tool-extended sensing, where a rod is touched is encoded pre-neuronally by patterns of vibration (i.e., vibratory motifs; Figures S1E and S1F). When transiently contacting an object, specific resonant modes (100–1,000 Hz for long wooden rods) are selectively excited, giving rise to vibratory motifs that unequivocally encode touch location [7]. These rapid oscillations are superimposed onto a slowly evolving rigid motion that places a load on the participant's fingers and wrist. Given that the somatosensory system is sensitive to both slow-varying loads (via proprioception) and rapid vibrations imposed to the hand (via touch), these two signals are difficult to disentangle experimentally.

To adjudicate between the contribution of each aspect of the mechanical signal, we repeated experiment 1 with a deafferented participant (DC) who lost proprioception in her right upper limb (33% accuracy in clinical testing) following the resection of a tumor near the right medulla oblongata [29]. Importantly, light touch was largely spared in her right limb (100% accuracy). DC completed the EEG experiment while holding a rod in her deafferented hand and intact left hand (separate blocks). Her behavioral performance was good for both the intact (72%) and deafferented (77%) limbs. Crucially, her neural dynamics exhibited the observed repetition suppression for both limbs, with a magnitude comparable to that of the healthy participants (Figures 1F, 1I, and S2). Though not excluding possible contributions from slow varying rigid motion (when available), this result strongly suggests that the observed suppression was largely driven by information encoded by vibrations.

Processing of Vibratory Motifs Is Temporally Efficient

We used a biologically plausible skin-neuron model [8] to quantify how efficiently the brain extracts touch location on a tool. According to principles of efficient coding, sensory cortices attempt to rapidly and sparsely represent the spatiotemporal statistics of the natural environment with minimal information loss [30]. DC's results suggest that the brain uses vibratory motifs to extract contact location on a rod. It has been hypothesized that the spiking patterns of Pacinian afferents encode object-to-object contact during tool use [31], a claim that we found model-based evidence for [7]. This temporal code must be decoded in somatosensory processing regions, perhaps as early as the cuneate nucleus [32].

We derived an estimate of "maximal efficiency" by quantifying the time course of location encoding in a simulated population of Pacinian afferents in the hand (Figures 2A and 2B). Support-vector machine (SVM) classification revealed a temporal code that was unambiguous about contact location within 20 ms (Figure 2C). This code was efficient, corresponding to 4.6 ± 1.7 spikes per afferent. Taking into account the known conduction delays between first-order afferents and SI [21], this finding—along with our prior study [7]—suggests that location encoding within 35–40 ms would reflect an efficient representational scheme. The early suppression observed in experiment 1 (Figures 1D–1I) is consistent with this estimate. This suggests that somatosensory cortex views these temporal spike patterns as meaningful tactile features, allowing humans to efficiently use a rod as an extended sensor.

Rapid Processing of Contact Location on the Arm

To identify when touch location on the body is processed, we conducted a second EEG experiment with ten participants from experiment 1. In this experiment, touch was applied at two locations on the ventral surface of the forearm (Figure 3A). We found significant repetition suppression effects corresponding to a cluster extending 44–144 ms after contact ($p = 0.005$; Figures 3B and 3C; Table S2). Suppression within this time window was found in almost all ten participants (Figure 3D) and spanned the two processing stages observed in experiment 1. This timing is in line with previous studies that have identified location-based suppression following touch on the body, including the arm [18].

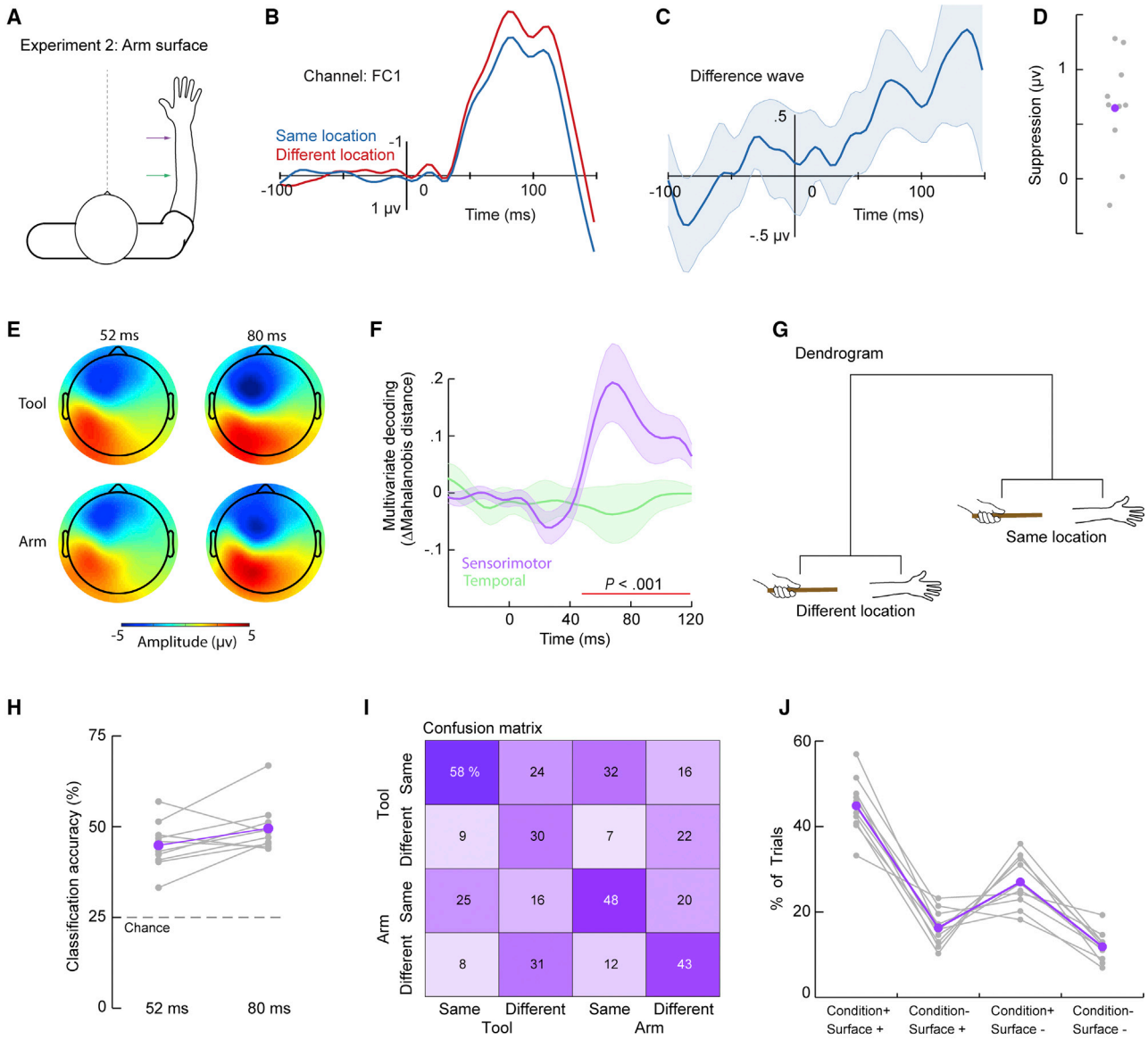

Figure 3. Similar Processing of Touch Location on the Arm and Tool

(A) Participants performed the exact paradigm as experiment 1 (Figures 1A–1C) with the exception that the stimulated surface was the arm.

(B) As with the first experiment, we found a significant reduction in SEP amplitude (between 52 and 144 ms) when the hit was in the same location on the arm (blue) compared to a different location (red).

(C) The time course of this suppression is more evident in the difference wave. Shaded areas represent the 95% confidence interval.

(D) We found suppression in the majority of participants (8 out of 10).

(E) Scalp topographies at early (52 ms) and late (80 ms) time points for touch on the tool (top row) and arm (bottom). To illustrate the general similarity between surfaces, we have collapsed scalp topographies across both the same and different conditions.

(F) Cross-surface multivariate decoding of suppression for each participant (n = 10) and at several time points (−40 to 120 ms). Decoding is expressed as the difference in the Mahalanobis distance between matching and non-matching trial conditions (i.e., same location versus different location). For sensorimotor channels (purple), we observed a significant cluster ($p < 0.001$; red line) of positive similarity between suppression on the tool and arm starting at 52 ms and continuing throughout our trial window. No significance was found for temporal channels (green). Shaded areas represent ±1 SEM for decoding across participants.

(G) Hierarchical clustering grouped neural responses by trial condition and not by surface touched.

(H) SVM classification accuracy for both early and late time points were significantly greater than chance (dashed gray line).

(I) Confusion matrix for classifier trained on the early time point (52 ms). Numbers correspond to the percentage of time the classifier chose that trial type.

(J) For ease of interpretation, we deconstructed the confusion matrix (early time point) into all categories of classifications. This includes accurate classification (condition+; surface+) and the three types of misclassifications. The majority of misclassifications were based on shared trial condition, not shared surface. See also Figures S3 and S4 and Table S2.

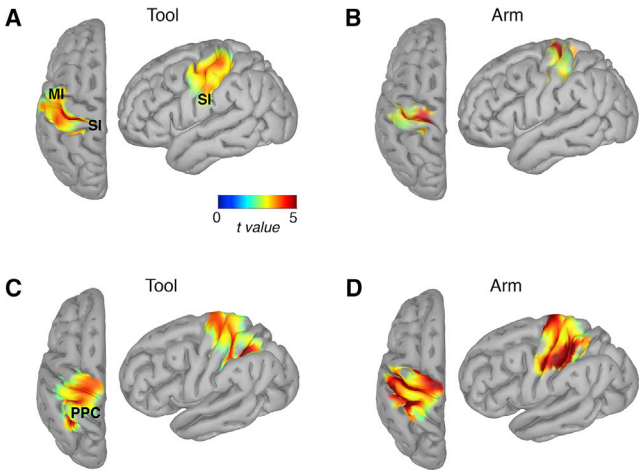

Figure 4. Neural Correlates of Touch Location on a Tool and Forearm

(A and B) Suppression shortly after contact (52 ms) on the rod (A) and arm (B) was confined to primary somatosensory and motor cortices.

(C and D) Activity 80 ms after contact on the rod (C) and arm (D) then spread to nearly identical regions in the posterior parietal cortex.

See also Figure S4.

Despite differences in the structure of the earliest somatosensory evoked potentials (SEPs) following touch on the rod and tool (Figure S3), the suppression observed across experiments was not significantly different ($p > 0.2$). The similarity between surfaces was also evident when inspecting the scalp topographies for both surfaces (Figure 3E), suggestive of similar neural dynamics. When interpreting these results, it is crucial to recall that the peripheral neural codes carrying information about where a rod or arm is touched are likely different: our modeling results suggest that where a rod is touched is represented by a spike-timing code (Figure 2) [7], whereas where the arm is touched is assumed to be represented by a place code [33]. Therefore, though not all early cortical responses are identical between touch on the arm and tool, the observed temporal overlap of suppression between surfaces suggests that the somatosensory cortex resolves these basic coding differences relatively early.

Similar Neural Dynamics Reflect the Processing of Touch Location on a Tool and Arm

We used multivariate analyses to better test the hypothesis that the brain uses similar processing stages for localizing touch on the arm and tool. First, using a representational decoding approach [34], we investigated whether the suppression observed in the arm dataset could predict the suppression observed in the tool dataset. We found statistically significant cross-surface decoding from cortical activity over sensorimotor channels starting within 52 ms of touch on either surface ($p < 0.001$; Figure 3F); decoding was not possible from channels over temporal cortex. Furthermore, hierarchical clustering grouped neural responses by trial condition (i.e., same, different location) and not touched surface (Figure 3G).

We trained an SVM to distinguish between all four trial types, grouped by both surface and trial condition. Significant classification accuracy (>25%) was found for both early (52 ms; accuracy: 44.8% ± 2.1%; one-sample t test: $p < 0.001$) and late (80 ms; accuracy: 49.5% ± 2.1%; one-sample t test: $p < 0.001$) neural responses (Figure 3H). We then characterized the types of misclassifications in the confusion matrix at both time points (Figures 3I and S4A–S4C). The SVM was more likely to identify the correct trial condition than the correct surface (Figure 3J; both $p < 0.05$). In sum, these results reveal the rapid emergence of statistically similar repetition suppression in the somatosensory system following touch on the arm and tool.

Similar Cortical Sources Localize Touch on a Tool and Arm

Finally, we compared the cortical sources for localizing touch on each surface. For the tool (Figure 4A) and the arm alike (Figure 4B), the earliest stages of shared suppression (52 ms) were localized in the hand and arm regions of SI and MI ($p < 0.05$; false discovery rate [FDR] corrected), respectively. The suppression in SI during tool sensing may reflect the efficient detection of a location-specific tactile feature (i.e., vibratory motifs). Alternatively, given the results of our multivariate analyses, the observed suppression may reflect a point in time when SI has already extracted touch location from motifs. This would suggest that SI can resolve differences in peripheral neural codes and represent touch location on both the body and tool using a common format.

After primary sensorimotor regions, the processing of touch location for the tool (Figure 4C) and arm (Figure 4D) spread throughout the posterior parietal cortex (PPC). These regions construct higher level spatial representations [35, 36] and even represent hands and tools within a shared coordinate system [37, 38]. They thus play an important role in tool use [2, 39]. The current results suggest that the PPC is involved in deriving a spatial code for where a tool was touched. A direct comparison of both surfaces at this processing stage found several shared sources in SI, MI, and PPC (Figure S4D), consistent with our scalp-level multivariate analyses (Figures 3 and S4A–S4C).

General Discussion and Implications

Identifying the spatial boundaries of a cognitive system requires characterizing how neural activity couples the body with external objects during thinking, acting, and perceiving [40]. For humans, tool use is a textbook example of an extended body [2–7] because it marks a step in human evolution when our ancestors could act on their environments in ways otherwise impossible. We show that tools are fundamental to human behavior in a previously underappreciated way: they expand the *somatosensory boundaries* of our body at the neural level. Hence, rather than stopping at the skin, our results suggest that somatosensory processing extends beyond the nervous system to include the tools we use.

We propose that an elementary strategy the human brain uses to sense with tools consists in sharing similar primary sensory dynamics devoted to the body. This allows a tool to be used as an extended, non-neural sense organ that can efficiently probe the user's surroundings. This finding challenges the long-held view that portrays SI as a layered structure of low-level feature detectors. Instead, our finding suggests that SI dynamics

instantiate high-level sensorimotor models of an organism [41, 42], including biological and extended parts.

Is the ability to sense with a tool merely a human case of detecting substrate vibrations? Indeed, it is well known that many species take advantage of information transported by material substrates [9]. Though some processing aspects of extended sensing may apply to objects that cannot be manipulated, there are several reasons for viewing tool-extended sensing as a unique case. The dexterity and tactile sensitivity of the human hand, along with its corresponding neural machinery [43], likely evolved because they aided in the manipulation of tools [44]. Sensitivity to vibrations during tool use is largely attributed to Pacinian mechanoreceptors, which are critical for fine object manipulation [31]. Our results may thus reflect neural processes that developed for sensing with tools.

Unlike other instances of sensitivity to substrate vibrations, sensing with tools is a process that is most effective during active manipulation. When a blind person uses a cane to sense the environment, they adapt how the cane is gripped and swept against surfaces to optimize sensory feedback (e.g., vibrations), a strategy referred to as information self-structuring [45]. In our prior study, we found that fine-grained accuracy was significantly better during fully active compared to partially passive sensing [7]. Though the present study utilized a partially passive sensing mode (owing to experimental constraints), participants often reported selecting a grip that made it easier to discriminate between close and far hits (see also [7]). Thus, tool-extended sensing is an active process and not a passive pick-up of information.

The boundaries of somatosensory processing are a key theoretical question that has practical, real-world implications. A growing movement in bioengineering attempts to design "biomimetic" prosthetic limbs that provide somatosensory feedback to users, with limited—yet encouraging—success [46]. For a prosthetic device to provide rich perceptual interaction with the world, its wearer must be able to perceive and act upon tactile events across its entire surface. Tactile feedback is typically provided via invasive procedures, such as peripheral nerve stimulation [47] and intracortical microstimulation [48]. The present results suggest that a complementary, non-invasive means to restore sensory feedback would be to design prostheses that possess well-designed structural dynamics in response to interactions with touching objects. Optimized transmission of these vibratory dynamics could leverage the identified sensorimotor mechanisms for mapping touch on a tool to aid in the use of a prosthetic device as an extended sensor.

STAR★METHODS

Detailed methods are provided in the online version of this paper and include the following:

- KEY RESOURCES TABLE
- LEAD CONTACT AND MATERIALS AVAILABILITY
- EXPERIMENTAL MODEL AND SUBJECT DETAILS
- METHOD DETAILS
  - Experimental Setup
  - Delayed match-to-sample paradigm
  - Clinical testing and details for participant DC
  - Electroencephalographic (EEG) recording parameters
  - Preprocessing of the EEG data
  - Vibration recordings
  - Skin-neuron model
- QUANTIFICATION AND STATISTICAL ANALYSIS
  - Cluster-based analysis of EEG signals
  - Multivariate pattern decoding of EEG signals
  - Source reconstruction
  - Support vector classification of simulated spikes
- DATA AND CODE AVAILABILITY

SUPPLEMENTAL INFORMATION

Supplemental Information can be found online at https://doi.org/10.1016/j.cub.2019.10.043.

ACKNOWLEDGMENTS

We thank Frédéric Volland for his help constructing the experimental setup. This work was supported by an Fondation pour la Recherche Medicale Postdoctoral Fellowship SPF20160936329 to L.E.M., from ANR-16-CE28-0015 Developmental Tool Mastery to A.F. and V.H., from ANR BLIND_TOUCH 2019CE37 to A.F. and L.E.M., by a Leverhulme Trust Visiting Professorship Grant to V.H., and from IHU CeSaMe ANR-10-IBHU-0003, Defi Auton Sublima, and the James S. McDonnell Scholar Award to A.F. All work was performed within the framework of the LABEX CORTEX (ANR-11-LABX-0042) of Université de Lyon.

AUTHOR CONTRIBUTIONS

L.E.M., V.H., and A.F. conceived of the experimental idea. L.E.M. and A.F. designed the EEG experiments. L.E.M., C.F., and V.R. collected and analyzed the EEG data. L.E.M. designed and analyzed the neuronal modeling experiment. J.L. and S.B. performed the assessments for participant DC. E.K. and R.S. built the solenoid setup. L.E.M., N.B., V.H., and A.F. wrote the paper. All authors approved of the final submission.

DECLARATION OF INTERESTS

The authors declare no competing interests.

Received: May 22, 2019
Revised: September 30, 2019
Accepted: October 21, 2019
Published: December 5, 2019

REFERENCES

1. Clark, A. (2008). Supersizing the Mind: Embodiment, Action, and Cognitive Extension (Oxford University Press).
2. Iriki, A., Tanaka, M., and Iwamura, Y. (1996). Coding of modified body schema during tool use by macaque postcentral neurones. Neuroreport *7*, 2325–2330.
3. Umiltà, M.A., Escola, L., Intskirveli, I., Grammont, F., Rochat, M., Caruana, F., Jezzini, A., Gallese, V., and Rizzolatti, G. (2008). When pliers become fingers in the monkey motor system. Proc. Natl. Acad. Sci. USA *105*, 2209–2213.
4. Cardinali, L., Frassinetti, F., Brozzoli, C., Urquizar, C., Roy, A.C., and Farnè, A. (2009). Tool-use induces morphological updating of the body schema. Curr. Biol. *19*, R478–R479.
5. Miller, L.E., Cawley-Bennett, A., Longo, M.R., and Saygin, A.P. (2017). The recalibration of tactile perception during tool use is body-part specific. Exp. Brain Res. *235*, 2917–2926.

6. Martel, M., Cardinali, L., Roy, A.C., and Farnè, A. (2016). Tool-use: an open window into body representation and its plasticity. Cogn. Neuropsychol. *33*, 82–101.
7. Miller, L.E., Montroni, L., Koun, E., Salemme, R., Hayward, V., and Farnè, A. (2018). Sensing with tools extends somatosensory processing beyond the body. Nature *561*, 239–242.
8. Saal, H.P., Delhaye, B.P., Rayhaun, B.C., and Bensmaia, S.J. (2017). Simulating tactile signals from the whole hand with millisecond precision. Proc. Natl. Acad. Sci. USA *114*, E5693–E5702.
9. Burton, G. (1993). Non-neural extensions of haptic sensitivity. Ecol. Psychol. *5*, 105–124.
10. Japyassú, H.F., and Laland, K.N. (2017). Extended spider cognition. Anim. Cogn. *20*, 375–395.
11. Yamamoto, S., and Kitazawa, S. (2001). Sensation at the tips of invisible tools. Nat. Neurosci. *4*, 979–980.
12. Saig, A., Gordon, G., Assa, E., Arieli, A., and Ahissar, E. (2012). Motor-sensory confluence in tactile perception. J. Neurosci. *32*, 14022–14032.
13. Kilteni, K., and Ehrsson, H.H. (2017). Sensorimotor predictions and tool use: hand-held tools attenuate self-touch. Cognition *165*, 1–9.
14. Imamizu, H., Miyauchi, S., Tamada, T., Sasaki, Y., Takino, R., Pütz, B., Yoshioka, T., and Kawato, M. (2000). Human cerebellar activity reflecting an acquired internal model of a new tool. Nature *403*, 192–195.
15. Grill-Spector, K., Henson, R., and Martin, A. (2006). Repetition and the brain: neural models of stimulus-specific effects. Trends Cogn. Sci. *10*, 14–23.
16. Schendan, H.E., and Kutas, M. (2003). Time course of processes and representations supporting visual object identification and memory. J. Cogn. Neurosci. *15*, 111–135.
17. Tamè, L., Pavani, F., Papadelis, C., Farnè, A., and Braun, C. (2015). Early integration of bilateral touch in the primary somatosensory cortex. Hum. Brain Mapp. *36*, 1506–1523.
18. Shen, G., Smyk, N.J., Meltzoff, A.N., and Marshall, P.J. (2018). Neuropsychology of human body parts: Exploring categorical boundaries of tactile perception using somatosensory mismatch responses. J. Cogn. Neurosci. *30*, 1–12.
19. Van Pelt, S., Toni, I., Diedrichsen, J., and Medendorp, W.P. (2010). Repetition suppression dissociates spatial frames of reference in human saccade generation. J. Neurophysiol. *104*, 1239–1248.
20. Strömmer, J.M., Tarkka, I.M., and Astikainen, P. (2014). Somatosensory mismatch response in young and elderly adults. Front. Aging Neurosci. *6*, 293.
21. Eisen, A., and Elleker, G. (1980). Sensory nerve stimulation and evoked cerebral potentials. Neurology *30*, 1097–1105.
22. Allison, T., McCarthy, G., and Wood, C.C. (1992). The relationship between human long-latency somatosensory evoked potentials recorded from the cortical surface and from the scalp. Electroencephalogr. Clin. Neurophysiol. *84*, 301–314.
23. Cardini, F., Longo, M.R., and Haggard, P. (2011). Vision of the body modulates somatosensory intracortical inhibition. Cereb. Cortex *21*, 2014–2022.
24. Akatsuka, K., Wasaka, T., Nakata, H., Kida, T., Hoshiyama, M., Tamura, Y., and Kakigi, R. (2007). Objective examination for two-point stimulation using a somatosensory oddball paradigm: an MEG study. Clin. Neurophysiol. *118*, 403–411.
25. Cauller, L.J., and Kulics, A.T. (1991). The neural basis of the behaviorally relevant N1 component of the somatosensory-evoked potential in SI cortex of awake monkeys: evidence that backward cortical projections signal conscious touch sensation. Exp. Brain Res. *84*, 607–619.
26. Jones, S.R., Pritchett, D.L., Stufflebeam, S.M., Hämäläinen, M., and Moore, C.I. (2007). Neural correlates of tactile detection: a combined magnetoencephalography and biophysically based computational modeling study. J. Neurosci. *27*, 10751–10764.
27. Soto-Faraco, S., and Azañón, E. (2013). Electrophysiological correlates of tactile remapping. Neuropsychologia *51*, 1584–1594.
28. Nakata, H., Inui, K., Nishihira, Y., Hatta, A., Sakamoto, M., Kida, T., Wasaka, T., and Kakigi, R. (2004). Effects of a go/nogo task on event-related potentials following somatosensory stimulation. Clin. Neurophysiol. *115*, 361–368.
29. Cardinali, L., Brozzoli, C., Luauté, J., Roy, A.C., and Farnè, A. (2016). Proprioception is necessary for body schema plasticity: evidence from a deafferented patient. Front. Hum. Neurosci. *10*, 272.
30. Simoncelli, E.P., and Olshausen, B.A. (2001). Natural image statistics and neural representation. Annu. Rev. Neurosci. *24*, 1193–1216.
31. Johansson, R.S., and Flanagan, J.R. (2009). Coding and use of tactile signals from the fingertips in object manipulation tasks. Nat. Rev. Neurosci. *10*, 345–359.
32. Jörntell, H., Bengtsson, F., Geborek, P., Spanne, A., Terekhov, A.V., and Hayward, V. (2014). Segregation of tactile input features in neurons of the cuneate nucleus. Neuron *83*, 1444–1452.
33. Sanchez Panchuelo, R.M., Ackerley, R., Glover, P.M., Bowtell, R.W., Wessberg, J., Francis, S.T., and Mcglone, F. (2016). Mapping quantal touch using 7 Tesla functional magnetic resonance imaging and single-unit intraneural microstimulation. eLife *5*, e12812.
34. van Ede, F., Chekroud, S.R., Stokes, M.G., and Nobre, A.C. (2019). Concurrent visual and motor selection during visual working memory guided action. Nat. Neurosci. *22*, 477–483.
35. Bolognini, N., and Maravita, A. (2007). Proprioceptive alignment of visual and somatosensory maps in the posterior parietal cortex. Curr. Biol. *17*, 1890–1895.
36. Buchholz, V.N., Jensen, O., and Medendorp, W.P. (2011). Multiple reference frames in cortical oscillatory activity during tactile remapping for saccades. J. Neurosci. *31*, 16864–16871.
37. Naito, E., and Ehrsson, H.H. (2006). Somatic sensation of hand-object interactive movement is associated with activity in the left inferior parietal cortex. J. Neurosci. *26*, 3783–3790.
38. Naito, E., Scheperjans, F., Eickhoff, S.B., Amunts, K., Roland, P.E., Zilles, K., and Ehrsson, H.H. (2008). Human superior parietal lobule is involved in somatic perception of bimanual interaction with an external object. J. Neurophysiol. *99*, 695–703.
39. Johnson-Frey, S.H. (2004). The neural bases of complex tool use in humans. Trends Cogn. Sci. *8*, 71–78.
40. Chiel, H.J., and Beer, R.D. (1997). The brain has a body: adaptive behavior emerges from interactions of nervous system, body and environment. Trends Neurosci. *20*, 553–557.
41. Brecht, M. (2017). The body model theory of somatosensory cortex. Neuron *94*, 985–992.
42. Giurgola, S., Pisoni, A., Maravita, A., Vallar, G., and Bolognini, N. (2019). Somatosensory cortical representation of the body size. Hum. Brain Mapp. *40*, 3534–3547.
43. Peeters, R., Simone, L., Nelissen, K., Fabbri-Destro, M., Vanduffel, W., Rizzolatti, G., and Orban, G.A. (2009). The representation of tool use in humans and monkeys: common and uniquely human features. J. Neurosci. *29*, 11523–11539.
44. Young, R.W. (2003). Evolution of the human hand: the role of throwing and clubbing. J. Anat. *202*, 165–174.
45. Lungarella, M., and Sporns, O. (2006). Mapping information flow in sensorimotor networks. PLoS Comput. Biol. *2*, e144.
46. Bensmaia, S.J., and Miller, L.E. (2014). Restoring sensorimotor function through intracortical interfaces: progress and looming challenges. Nat. Rev. Neurosci. *15*, 313–325.
47. Valle, G., Mazzoni, A., Iberite, F., D'Anna, E., Strauss, I., Granata, G., Controzzi, M., Clemente, F., Rognini, G., Cipriani, C., et al. (2018). Biomimetic intraneural sensory feedback enhances sensation naturalness, tactile sensitivity, and manual dexterity in a bidirectional prosthesis. Neuron *100*, 37–45.e7.

48. Flesher, S.N., Collinger, J.L., Foldes, S.T., Weiss, J.M., Downey, J.E., Tyler-Kabara, E.C., Bensmaia, S.J., Schwartz, A.B., Boninger, M.L., and Gaunt, R.A. (2016). Intracortical microstimulation of human somatosensory cortex. Sci. Transl. Med. *8*, 361ra141.

49. Delorme, A., and Makeig, S. (2004). EEGLAB: an open source toolbox for analysis of single-trial EEG dynamics including independent component analysis. J. Neurosci. Methods *134*, 9–21.

50. Tadel, F., Baillet, S., Mosher, J.C., Pantazis, D., and Leahy, R.M. (2011). Brainstorm: a user-friendly application for MEG/EEG analysis. Comput. Intell. Neurosci. *2011*, 879716.

51. R Development Core Team (2014). R: A language and environment for statistical computing (R Foundation for Statistical Computing).

52. Winward, C.E., Halligan, P.W., and Wade, D.T. (2002). The Rivermead Assessment of Somatosensory Performance (RASP): standardization and reliability data. Clin. Rehabil. *16*, 523–533.

53. Makeig, S., Bell, A.J., Jung, T.P., and Sejnowski, T.J. (1996). Independent component analysis of electroencephalographic data. Adv. Neural Inf. Process. *8*, 145–151.

54. Chaumon, M., Bishop, D.V.M., and Busch, N.A. (2015). A practical guide to the selection of independent components of the electroencephalogram for artifact correction. J. Neurosci. Methods *250*, 47–63.

55. Maris, E., and Oostenveld, R. (2007). Nonparametric statistical testing of EEG- and MEG-data. J. Neurosci. Methods *164*, 177–190.

56. Cortes, C., and Vapnik, V. (1995). Support-vector networks. Mach. Learn. *20*, 273–297.

57. Meyer, D., Dimitriadou, E., Hornik, K., Weingessel, A., Leisch, F., Chang, C.C., and Lin, C.C. (2015). e1071: Misc functions of the department of statistics, probability theory group (formerly: E1071), TU Wien. R package version 1.6-7.

58. Chang, C.C., and Lin, C.J. (2011). LIBSVM: a library for support vector machines. ACM Trans. Intell. Syst. Technol. *2*, 27.

59. Pascual-Marqui, R.D. (2002). Standardized low-resolution brain electromagnetic tomography (sLORETA): technical details. Methods Find. Exp. Clin. Pharmacol. *24* (*Suppl D*), 5–12.

60. Gramfort, A., Papadopoulo, T., Olivi, E., and Clerc, M. (2010). OpenMEEG: opensource software for quasistatic bioelectromagnetics. Biomed. Eng. Online *9*, 45.

STAR★METHODS

KEY RESOURCES TABLE

REAGENT or RESOURCE	SOURCE	IDENTIFIER
Deposited Data		
EEG experiments 1-2 and TouchSim simulations	Open Science Framework	https://osf.io/c4qmr/
Software and Algorithms		
MATLAB 2017b	The MathWorks	RRID:SCR_001622
EEGLab Toolbox	[49]	https://sccn.ucsd.edu/eeglab; RRID:SCR_007292
Brainstorm Toolbox	[50]	https://neuroimage.usc.edu/brainstorm; RRID:SCR_001761
TouchSim	[8]	https://bensmaialab.org/download/
R version 3.2.3	[51]	RRID:SCR_001905

LEAD CONTACT AND MATERIALS AVAILABILITY

Further information and requests for resources should be directed to and will be fulfilled by the Lead Contact, Luke E. Miller (L.Miller@donders.ru.nl). This study did not generate new unique reagents.

EXPERIMENTAL MODEL AND SUBJECT DETAILS

16 right-handed subjects (mean age: 26.5 years, range 20 to 34 years, 5 males) free of any known sensory, perceptual, or motor disorders, volunteered to participate in Experiment 1. Ten of these participants also completed Experiment 2. A neurological patient (DC; female, 50 years of age) also completed Experiment 1. All subjects provided written informed consent according to national guidelines of the ethics committee (CPP SUD EST IV).

METHOD DETAILS

Experimental Setup

In Experiment 1, Participants sat in a chair with their right arm placed on an adjustable armrest. A wooden rod (length: 100 cm; cross-sectional radius: 0.75 cm) was held in their right hand, with the tip of the stick resting on a support so that it would stay stable and parallel to the participant's midline. A fixation cross was displayed on a computer screen ~100 cm in front of the participant. A left foot double-pedal (Leptron Footswitch 548561) was used to make responses in the task (see below).

The rod was contacted with solenoids (Mecalectro 8.19.AB.83) at two different location (see Figure 1A): ~16 cm from the hand (close location) and ~63 cm from the hand (far location). The solenoids were powered with 36W in order to achieve a sufficient impact level and were controlled via custom MATLAB code. Each had an identical acceleration profile, ensuring that contact force (~14 N) did not vary from trial-to-trial. Furthermore, the acceleration onset of the solenoid was controlled with sub-millisecond precision (SD of acceleration onset: 0.26 ms), guaranteeing good time-locking for the EEG analysis (see below). All solenoids were secured by adjustable tripods, which were used to place the solenoid 1 cm below the surface of the rod. To ensure uniform and consistent contact between solenoids and the body of the rod, a plastic disc (4 cm diameter) was added at the tip of each solenoid's metal point.

Two precautions were taken to mask the sound generated by the solenoids: (i) white noise was played continuously over noise-cancelling earphones (Bose QuietComfort 20) at a level that made the solenoids almost inaudible; (ii) a 'decoy' solenoid was placed next to the rod and in between the other two solenoids so that the activation of each solenoid was always accompanied by an activation of the decoy, further obscuring auditory cues to solenoid position. All solenoids were supported by adjustable tripods at the same height. Visual cues were prevented by spreading a black sheet between the screen and subjects' neck to cover their hands and the stick.

The experimental setup was almost exactly the same as Experiment 1. Participants sat in a chair with their right elbow and hand each placed on an armrest. Stimulation was applied to the ventral surface of their right forearm, which was position between each arm rest. As with the prior experiment, the solenoids were positioned at two locations, ~5 cm from the crook of the arm and ~5 cm from the wrist, and 1 cm below the surface.

Delayed match-to-sample paradigm

Participants performed a delayed match-to-sample task (DMS) whereby they had to decide whether two mechanical stimulations were in the same or different location on either the rod (Experiment 1) or the arm (Experiment 2). Specifically, participants were

instructed to report whether the two contacts were in the same or a different location, using foot pedals placed under their left foot (i.e., ipsilateral to the site of stimulation). When the two locations of contact were different, participants made no overt response. When they were in the same location, we required them to make explicit judgments about whether they were close to the hand (raising their heal) or far from the hand (raising their toe). This ensured that our paradigm did not fall prey to the known criterion effects in based same versus different psychophysical tasks. Furthermore, no feedback was ever given to participants on whether their responses were correct or incorrect, ensuring that they could not learn arbitrary rules to distinguish close or far. All stimulus presentation and behavioral response collection was controlled via custom scripts in MATLAB (MathWorks).

The structure of each trial was as follows. Each trial began with a fixation cross presented at the center of the computer screen, which blinked after 1000 ms to inform the participants that a contact was coming soon and to therefore pay attention. After a delay period (between 1000-1500 ms, randomly chosen from a uniform distribution), mechanical stimulation was applied to the experimental surface (i.e., rod or arm) at one of the two locations (close or far; pseudo-randomly chosen). During a retention period, participants kept the location of contact in working memory (between 2000-2500 ms, randomly chosen from a uniform distribution); this retention period ended with the application of the second stimulus (location chosen pseudo-randomly). Participants then decided whether the second hit was in the same location as the first and kept this decision in mind during a further delay period (between 1000-1500 ms, randomly chosen from a uniform distribution). This delay period ended when the fixation cross changed to an 'X', signifying to the subject to make a response (see above). The 'X' turned back into a fixation cross just after the response was made, or after 2000 ms if no response, and the next trial began.

Subjects performed four blocks of 100 trials each (400 trials in total), in which stimulus location was pseudo-randomly interleaved for each hit. Thus, there were 200 contacts per location for each of the two hits (400 close and 400 far contacts in total). Furthermore, on half of the trials the two hits were in the same location and on the other half the two hits were in different locations. Each trial lasted between 5000 and 8500 ms. A brief rest period was provided between blocks during which the subjects could move their hands and eyes freely. For two participants in each experiment, one block of data was not recorded due to experimenter error; their full dataset therefore only contains three blocks.

Clinical testing and details for participant DC

We have previously completed a tool-use experiment with participant DC [29]. DC is a right-handed 50-year old woman who underwent surgery in March 2006 to remove a vascular tumor in the proximity of the right medulla oblongata. Following surgery, DC lost proprioception and kinaesthesia in her right upper limb, which remains deafferented to this day. Light touch on her right upper limb is largely spared. She currently prefers manipulating objects and use tools with her right hand (self-report and Edinburgh Handedness Index), and often compensates with visual feedback. The sensorimotor functions of all other limbs were unaffected by the surgery.

Clinical examination with the Rivermead Assessment of Somatosensory Performance [52] was performed prior to her inclusion in the present study. This test confirmed that, for both hands, she could perfectly discriminate sharp/dull probes, detect surface pressure, and localize touches (100% accuracy). Her ability to discriminate proprioceptive movements of her elbow, wrist, and thumb were perfect for her left upper limb (100% accuracy). On the contrary, she was highly impaired when discriminating proprioceptive movements of three joints (i.e., elbow, wrist, and thumb) for her right upper limb (33% accuracy).

Participant DC completed the procedures from Experiment 1 with both her intact (left) and deafferented (right) hand in separate blocks (block order: left, right, right, left). The experimental procedures were identical to described above. In debriefing, DC reported that she did not feel her wrist moving during the experiment.

Electroencephalographic (EEG) recording parameters

EEG data were recorded continuously using a 65 channel ActiCap system (Brain Products). Horizontal and vertical electro-oculograms (EOGs) were recorded using electrodes placed below the left eye, and near the outer canthi of the right eye. Impedance of all electrodes was kept at < 20 kΩ. FCz served as the reference during recording. EEG and EOG signals were low-pass filtered online at 0.1 Hz, sampled at 2500 Hz, and then saved to a disk.

Preprocessing of the EEG data

EEG signals were preprocessed using the EEGLab Toolbox [49]. The preprocessing steps for each participant were as follows: We appended all four blocks of the experiment into a single dataset, resampled the signal at 250 Hz, and high-pass filtered at 1 Hz. We then epoched the data into a time window of 3 s, 1 s before and 2 s after the hit (time zero). We then isolated epochs related to the second hit, as this was the focus of our analysis (see below); each epoch was categorized as reflecting the same location as the first hit ('same' condition) or a different location ('different' condition). Next, we removed signal artifacts with two steps: First, we removed eye blinks and horizontal eye movements from the signal using independent components analysis [53] and a semi-automated algorithm called SASICA [54]. Second, we excluded the first ten trials of the experiment, trials that were interrupted by the experimenter, all trials where subjects answered incorrectly, and manually rejected trials that were contaminated by muscle artifacts or other forms of signal noise. In all, this led to a mean exclusion of 35.5 trials in Experiment 1 (range: 14–56) and 24.1 trials in Experiment 2 (range: 12-43). Next, we used the EEGLab function *pop_reref* to add FCz (the online reference) back into the dataset. Finally, we re-referenced the data to the average voltage across the scalp and re-epoched the data into a time window of 250 ms, –100 ms before

and 150 ms after the hit. We chose this time window because it captures three mid-latency somatosensory evoked potentials (SEPs) related to the early stages of perceptual processing [22], the P50, N80 and P100.

Vibration recordings

We previously demonstrated that information about impact location is initially encoded by the modal response of a rod when contacted [7]. We recorded these vibrations in order to estimate how mechanoreceptors in the hand respond to impact at the two locations in Experiment 1. All vibrations were recorded using a miniature tri-axis analog accelerometer (Analog Devices; Model ADXL335), which have low mass (40.0 mg), a wide frequency bandwidth (0–1,600 Hz in X and Y; 0–550 Hz in Z), and high dynamic range (−3.6 to 3.6 g).

Vibrations were recorded from the base of the tool shaft as one of the authors (V.R.) held the rod in place. The modal response of the rod was measured forty times for each location. We restricted the recording to the Z axis as this contained the bulk of the impact response. The signal was digitized with a 14-bit resolution and sampled at a frequency of 2 kHz over a three-second window using a data acquisition device (National Instruments; Model USB-6009). We then converted the signal into three temporal derivatives (acceleration, velocity, and displacement) and high-pass filtered it at 100 Hz using a 3rd order zero-phase Butterworth FIR filter. All data was recorded and processed using MATLAB 2017b (The MathWorks).

Skin-neuron model

Pacinian mechanoreceptors in the hand have previously been proposed to play a role in encoding vibrations during tool-surface contact [31]. We recently provided evidence, using a biologically plausible computational skin-neuron model (TouchSim; [8]), that they re-encode where a tool has been touched [7]. MATLAB code to implement the model is freely available online (http://bensmaialab.org/download/). The reader should refer to the original article for an in-depth treatment of the methods and model validation.

We used TouchSim to simulate the responses of a population of Pacinian mechanoreceptors (286 in total) to the vibrations described above. The population was confined to skin surfaces that are tangential to the force of impact when holding the rod. The vibration on each trial (see above) was used as the input for each mechanoreceptor in the population. To more realistically simulate the mechanoreceptors, the temporal profile of their responses included stochastic noise and considered known mechanical and spiking delays. We then derived the population-level response pattern by summing the spiking of each individual mechanoreceptor.

QUANTIFICATION AND STATISTICAL ANALYSIS

Cluster-based analysis of EEG signals

The goal of each experiment was to identify time windows where the amplitude of SEPs was modulated by whether the location of contact was repeated or not (see Main Text). We hypothesized that the evoked response to the second hit would be smaller when the stimulus was at the same location as the first (i.e., 'same' condition), compared to when it was at a different location (i.e., 'different' condition). We therefore focused our analysis on the evoked responses to the second stimulus presentation. Identical results were found when this procedure was performed on the two contact locations separately (data not shown); we therefore combined them into a single dataset for the final analysis. To identify time windows of suppression, we used a nonparametric cluster-based permutation test [55], a popular data-driven approach that robustly controls for the multiple comparison problem inherent in M/EEG analysis. We focused this analysis on electrodes over temporal and sensorimotor regions contralateral to the stimulation: P7, P5, P3, P1, Pz, TP9, TP7, CP5, CP3, CP1, CPz, T7, C5, C3, C1, Cz, FT9, FT7, FC5, FC3, FC1, FCz, F7, F5, F3, F1, and Fz. The sensorimotor electrodes are the most common sites of the three SEPs corresponding to the chosen time window [22] and the temporal electrodes served as neutral electrodes where no suppression was expected.

Multivariate pattern decoding of EEG signals

Decoding was performed on the datasets from the ten participants that took part in both Experiment 1 and 2. The trial-by-trial EEG signal is dominated by low-frequency oscillations, which swamp the evoked responses. Therefore, in order to place greater emphasis on the evoked SEPs, we subtracted the EEG following the first hit from the second hit on every trial. Trials were then classified by the two above-mentioned trial conditions: Same and Different.

Representational distance approach

To test the hypothesis that similar processing stages are used to localize touch on an arm and tool, we compared the similarity of the multivariate neural patterns of suppression for both surfaces at each time point (−40 to 120 ms after touch) using the Mahalanobis distance (MD) metric [34]. All trials in both the tool and arm datasets were divided into the conditions 'same location' and 'different location'. Then, for each trial in the participant's tool dataset, we calculated its MD from the average of all trials in the participant's arm dataset whose condition was either matching or non-matching. For example, a trial in the 'same' condition from the tool dataset could be compared against the average of the 'same' condition (match) or the 'different' condition (non-matching) in the arm dataset. The degree of decoding for each time point was then quantified by subtracting the condition-matched MD from the condition-mismatched MD.

If the multivariate neural patterns of suppression in the arm dataset were in fact predictive of the patterns of suppression in the tool dataset, per our hypothesis, the condition-matched MD should yield smaller values than the condition-mismatched MD. We assessed this using the nonparametric cluster-based permutation test described above. Prior to this analysis, the trial-averaged MD values for each participant were smoothed using a Gaussian-kernel with a standard deviation of 8 ms. This approach increases the sensitivity of the analysis [34] and did not have an effect on our pattern of results. We restricted the present analysis (and therefore the multivariate patterns) to nine of the sensorimotor channels from the significant cluster in Experiment 1 (CP3, CP1, CPz, C3, C1, Cz, FC3, FC1, FCz) and seven ventral electrodes where no significant classification was expected (P7, TP9, TP7, T7, FT9, FT7, F7).

Hierarchical clustering

The full dataset for each participant contains four distinct trial types that are derived from the combinations of trial condition and the surface touched. We used hierarchical clustering to assess their representational similarity. The Euclidean distance between the trial-average neural patterns for each trial type was calculated for each participant. We then averaged the matrix of Euclidean distances across all participants and clustered the data using the *hclust* function in R version 3.2.3 [51]. This was done for two time points: (i) the earliest time point (52 ms) of significant cross-surface decoding described above; (ii) a later time point (80 ms) corresponding to the peak of the N80 (Figures S1 and S3). We restricted the present analysis to nine of the sensorimotor channels from the significant cluster in Experiment 1 (CP3, CP1, CPz, C3, C1, Cz, FC3, FC1, FCz).

Support vector classification

For each participant, we attempted to classify the four distinct trial types in their full dataset using a support vector machine (SVM) [56] with a radial basis kernel. Our classification scheme used 5-fold cross validation. Thus, we trained the classifier on four subsamples of the data (i.e., 80% of the trials) and tested classifier performance on the leftover subsample (i.e., the remaining 20% of the trials). Each fold had an equal number of items per trial type. The hyperparameters of the SVM, C and γ, were tuned using grid search; tuning occurred separately for each of the five classification iterations. The features for classification were the neural patterns of suppression for each of the two time points mentioned above (i.e., 52 and 80 ms). Classification was performed using the e1071 package [57] and its interface with LIBSVM [58]. This was implemented with R version 3.2.3 [51]. Chance classification (i.e., random guessing) was 25%. Classification was done separately for each participant. We restricted the present analysis to nine of the sensorimotor channels from the significant cluster in Experiment 1 (CP3, CP1, CPz, C3, C1, Cz, FC3, FC1, FCz).

To further explore the performance of the classifier, we assessed the confusion matrix for each participant. There were four possible types of classifier judgments. The classifier could be completely accurate about both condition and surface (condition+, surface+). The classifier could also produce three types of possible misclassifications: (i) accurate about surface only (condition-, surface+); (ii) accurate about condition only (condition+, surface-), and (iii) fully inaccurate (condition-, surface-). Different proportions of misclassification are informative about which categories are considered most similar and distinct by the classifier.

Source reconstruction

The cortical sources underlying the observed repetition suppression in both experiments were estimated using Standardized Low Resolution Brain Electromagnetic Tomography (sLORETA) [59], which approximates the generators underlying a given scalp topography by finding a discrete solution to the inverse problem. A boundary element method (OpenMEEG) was used to create a realistic head model (15000 vertices) to constrain source reconstruction [60]. This process was implemented using the Brainstorm toolbox [50], which is freely available for download online under the GNU general public license (http://neuroimage.usc.edu/brainstorm). Sources were reconstructed separately for each experimental condition ('same' and 'different') and were statistically compared using a paired permutation-based t test (1000 repetitions) at the group-level (FDR corrected at $p < 0.05$). Given prior studies on the sources between 40 and 100 ms after stimulation [22, 23, 26, 27], we constrained our analyses to a region-of-interest covering contralateral MI, SI, and the PPC (1300 vertices). Our analysis focused on two time points in the observed windows of suppression discussed above: 52 and 80 ms. Qualitatively similar results were found when using a cluster-based approach to source reconstruction (data not shown).

We further compared the sources for each surface, tool and arm, in the ten participants who completed both experiments. We first investigated the interaction between condition ('same', 'different') and surface (tool, arm) by using the above methods to compare the sources of suppression (i.e., the arithmetic difference between both conditions) for both surfaces. Given that this analysis yielded no results, we combined the data from both experiments into a single dataset in order to identify regions that coded for contact location on both the tool and arm.

Support vector classification of simulated spikes

We sought to derive a theoretical lower bound on how efficiently the brain could extract where a rod was touched. This involved three steps: (i) recording the rod's modal responses to being impacted (see above); (ii) simulating how this response is encoded by mechanoreceptors in the hand (see above); (iii) using machine learning to classify how quickly impact location emerges in mechanoreceptor spiking.

We classified impact location from the population response using a support vector machine (SVM) [56] with a radial basis kernel. Our classification scheme used 5-fold cross validation. Thus, we trained the classifier on four subsamples of the data (i.e., 80% of the trials) and tested classifier performance on the leftover subsample (i.e., the remaining 20% of the trials). Each fold had an equal

number of items per impact location. The hyperparameters of the SVM, C and γ, were tuned using grid search; tuning occurred separately for each of the five classification iterations. We specifically sought to characterize when a location-specific pattern emerged in the PC population's spiking pattern. The features for classification were therefore subsets of this population spiking across multiple temporal window sizes (5 to 50 ms, in steps of 1 ms). Classification was performed using the e1071 package [57] and its interface with LIBSVM [58]. This was implemented with R version 3.2.3 [51]. Chance classification (i.e., random guessing) was $\sim$50%.

DATA AND CODE AVAILABILITY

Data for the EEG experiments and skin-neuron modeling is available here (https://osf.io/c4qmr/). For privacy reasons, this does not include the data from participant DC. Additional requests should be sent to the Lead Contact, Luke E. Miller (L.Miller@donders.ru.nl).